Positrons vs electrons channeling in silicon crystal: energy levels, wave functions and quantum chaos manifestations

JINST

Published by IOP Publishing for Sissa Medialab

Received: *October 26, 2017*
Revised: *December 19, 2017*
Accepted: *December 28, 2017*
Published: *January 16, 2018*

XII International Symposium on Radiation from Relativistic Electrons in Periodic Structures — RREPS-17
18–22 September, 2017
DESY, Hamburg, Germany

Positrons vs electrons channeling in silicon crystal: energy levels, wave functions and quantum chaos manifestations

N.F. Shul'ga,[a,b] **V.V. Syshchenko,**[c,1] **A.I. Tarnovsky,**[c] **I.I. Solovyev**[c] **and A.Yu. Isupov**[d]

[a] *Akhiezer Institute for Theoretical Physics of the NSC "KIPT", Akademicheskaya Street, 1, Kharkov 61108, Ukraine*
[b] *V.N. Karazin National University, Svobody Square, 4, Kharkov 61022, Ukraine*
[c] *Belgorod State University, Pobedy Street, 85, Belgorod 308015, Russian Federation*
[d] *Laboratory of High Energy Physics (LHEP), Joint Institute for Nuclear Research (JINR), Dubna 141980, Russian Federation*

E-mail: syshch@yandex.ru

Abstract: The motion of fast electrons through the crystal during axial channeling could be regular and chaotic. The dynamical chaos in quantum systems manifests itself in both statistical properties of energy spectra and morphology of wave functions of the individual stationary states. In this report, we investigate the axial channeling of high and low energy electrons and positrons near [100] direction of a silicon crystal. This case is particularly interesting because of the fact that the chaotic motion domain occupies only a small part of the phase space for the channeling electrons whereas the motion of the channeling positrons is substantially chaotic for the almost all initial conditions. The energy levels of transverse motion, as well as the wave functions of the stationary states, have been computed numerically. The group theory methods had been used for classification of the computed eigenfunctions and identification of the non-degenerate and doubly degenerate energy levels. The channeling radiation spectrum for the low energy electrons has been also computed.

Keywords: Interaction of radiation with matter; Detector modelling and simulations I (interaction of radiation with matter, interaction of photons with matter, interaction of hadrons with matter, etc)

ArXiv ePrint: 1708.03667

[1] Corresponding author.

https://doi.org/10.1088/1748-0221/13/01/C01017

Contents

1 Introduction

The fast charged particles incident onto the crystal under a small angle to any crystallographic axis densely packed with atoms can perform the finite motion in the transverse plane known as the axial channeling [1, 2]. The particle motion in this case could be described with a good accuracy as the one in continuous potential of the atomic string. During motion in this potential the longitudinal particle momentum $p_{\|}$ is conserved, so the motion description is reduced to two-dimensional problem of motion in the transversal plane. This motion can be substantially quantum [1].

From the viewpoint of the dynamical systems theory, the channeling particle's motion could be either regular or chaotic. The quantum chaos theory [3–6] predicts qualitative difference for these alternatives. These differences have been demonstrated for the channeling electron in the semiclassical domain [7], where the energy levels density is high. Here we consider the opposite case when the total number of energy levels in the potential well is small.

2 Method and potential wells

The electron transversal motion in the atomic string continuous potential is described by the two-dimensional Schrödinger equation with Hamiltonian

$$\hat{H} = -(c^2\hbar^2/2E_{\|})\left[(\partial^2/\partial x^2) + (\partial^2/\partial y^2)\right] + U(x, y) \tag{2.1}$$

and the value $E_{\|}/c^2$ (here $E_{\|} = (m^2c^4 + p_{\|}^2c^2)^{1/2}$) instead of the particle mass [1]. The Hamiltonian eigenfunctions as well as the transverse energy $E_{\perp}$ eigenvalues are found numerically using the so-called spectral method [8, 9]; see details in [7]. Here we consider the particle's motion near direction of the atomic string [100] of the Si crystal. The continuous potential could be represented by the modified Lindhard potential [1]

$$U^{(1)}(x, y) = -U_0 \ln\left[1 + \beta R^2/(x^2 + y^2 + \alpha R^2)\right], \tag{2.2}$$

where $U_0 = 66.6\,\text{eV}$, $\alpha = 0.48$, $\beta = 1.5$, $R = 0.194$ Å (Thomas-Fermi radius). These strings form in the plane (100) the square lattice with the period $a \approx 1.92$ Å. The additional contributions from the eight closest neighboring strings lead to the following potential energy of the channeling electron:

$$U^{(-)}(x, y) = \sum_{i=-1}^{1} \sum_{j=-1}^{1} U^{(1)}(x - ia, y - ja) + 9.8083\ \text{eV}, \tag{2.3}$$

where the constant is added to achieve zero potential in the corners of the elementary cell.

The positrons can perform axial channeling near [100] direction due to small potential well formed near the center of the square cell with repulsive potentials $-U^{(1)}$ in the corners of the square:

$$\begin{aligned} U^{(+)}(x, y) = & -U^{(1)}(x - a/2, y - a/2) - U^{(1)}(x - a/2, y + a/2) \\ & -U^{(1)}(x + a/2, y - a/2) - U^{(1)}(x + a/2, y + a/2) - 7.9589\ \text{eV}, \end{aligned} \tag{2.4}$$

where the constant is chosen to achieve zero potential in the center of the cell.

So, the electrons channeling along [100] direction move in a weakly disturbed, almost axially symmetric potential. While their motion in this potential is regular for the most part, the dynamics of channeling positrons is mostly chaotic, that can be shown using Poincaré section method [1].

3 Results and discussion

The potential (2.3) in which the electron channels is the potential of the single string (2.2) weakly perturbed by the closest neighbors. The motion in the axially symmetric potential of the single string is integrable: the polar coordinates $r = \sqrt{x^2 + y^2}$ and $\varphi = \arctan(y/x)$ separates, and the Hamiltonian eigenfunctions split into the products of radial and angular parts. These eigenstates can be classified by two quantum numbers, the radial n_r and the orbital m. The $m = 0$ states are non degenerated; the $m \neq 0$ states are twice degenerate. The eigenfunctions of the real Hamiltonian without magnetic field and spin (like our (2.1)) always can be chosen real, hence we choose

$$\rho_{n_r,\,m}(r)\cos(m\varphi) \tag{3.1}$$

and

$$\rho_{n_r,\,m}(r)\sin(m\varphi) \tag{3.2}$$

as the basis functions for $m \neq 0$. The value m in this case manifests itself in the number of straight nodal lines $\psi(x, y) = 0$ travelling through the origin of coordinates (while the value n_r determines the number of circular nodal lines with the center in the origin), see figure 1.

The axial symmetry violation due to the perturbation from the neighbors partially breaks the degeneracy. The character of this partial splitting can be predicted using the group theory. The potential (2.3) possesses the symmetry of the square thus isomorphic to dihedral group D_4 (or C_{4v}). This group has four one-dimensional irreducible representations and one two-dimensional one, denoted A_1, A_2, B_1, B_2, E [10]. It appears [11] that the states (3.1) with $m = 4, 8, 12\ldots$ are transformed according to A_1 representation while the states (3.2) with the same m are transformed according to A_2 representation. Hence the perturbation shifts the energy eigenvalues in each of these state pair by the different values that leads to the energy level splitting. The levels with

2018 JINST 13 C01017

$m = 2, 6, 10 \ldots$ are split in the same way: the states (3.1) are the basic ones for B_1 representation while the states (3.2) form one-dimensional bases for B_2. The pairs of states (3.1)–(3.2) with odd m make the bases of the two-dimensional representation E, transforming into each other under D_4 group transformations, so the perturbation that possesses D_4 symmetry conserves their degeneration.

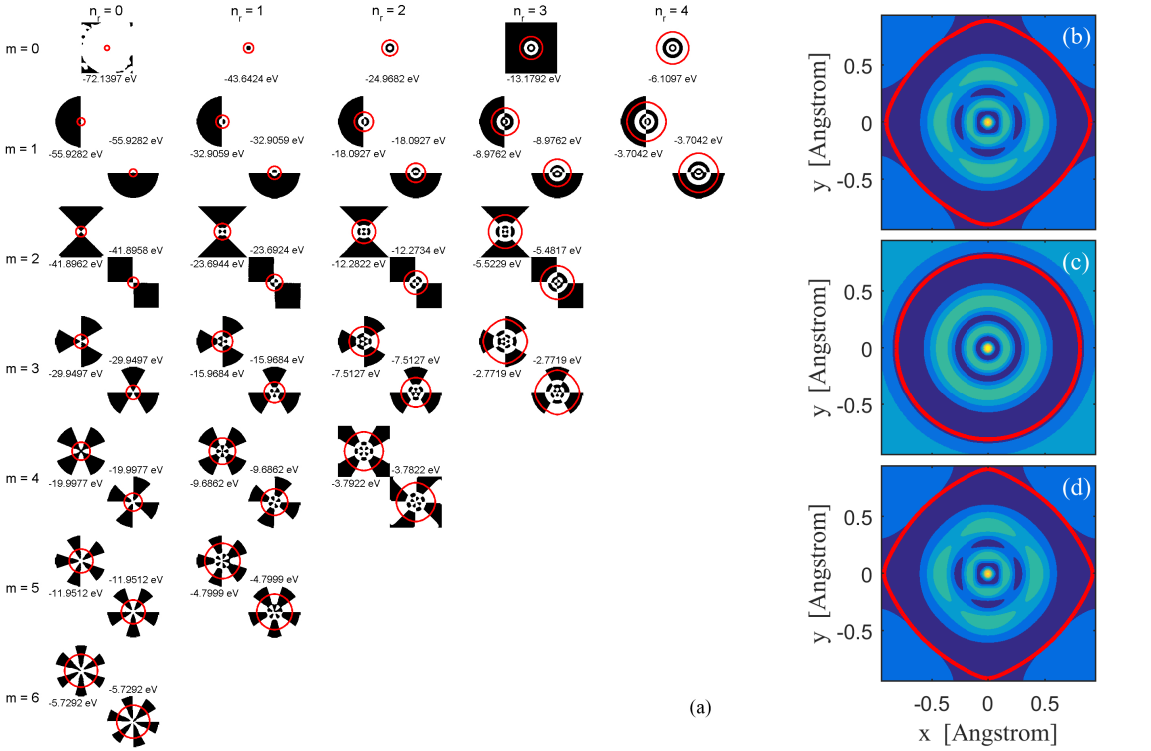

Figure 1. (a) Plots of the transverse motion eigenfunctions of $E_{\|} = 50\,\text{MeV}$ electron channeling along [100] axis with their $E_{\perp}$ eigenvalues (except the highest one), where black and white domains correspond to negative and positive values of the function. Red lines mark the classical border of motion $U^{(-)}(x, y) = E_{\perp}$. (b) The eigenfunction of the highest energy state $E_{\perp} = -2.3957\,\text{eV}$ of the electron channeling in the potential (2.3). (c) The analogous eigenfunction in the potential of the single string (2.2). (d) The same as in (b), but accounting the influence of 24 closest neighbors of the given string.

The physical origin of the level splitting lies in the follows. The wave functions in the pairs (3.1)–(3.2) differ from each other by the rotation on the angle $\pi/2m$. For even m, the finction (3.1) has its antinodes (that means maximal probability density) in the domains where the potential energy perturbation is maximal, while its counterpart (3.2) has its nodes in that places. So, the state (3.1) gets larger addition to its energy than the state (3.2). Hence this addition is negative we obtain sinking of the (3.1) states comparing to the (3.2) ones, see figure 1. On the other hand, for the (3.1)–(3.2) pairs with odd m the number of nodes and antinodes that fall on the perturbation with the symmetry of the square does not change under rotation on the angle $\pi/2m$, so the level degeneration conserves.

Violation of the axial symmetry in the upper part of the potential well (where the perturbation is maximal) manifests itself in the wave function structure: instead of the pure state $|n_r = 5, m = 0\rangle$ for the highest level (figure 1 (c)) we see the superposition of the states with orbital momenta 0 and 4; this feature cannot be seen in the pattern of the nodal lines $\psi(x, y) = 0$. Note that the

2018 JINST 13 C01017

next neighbor atomic strings lead to negligible influence on the potential and hence the electron's motion. It is clearly seen while comparing the figures 1 (b) and (d), where the wave functions of the same state computed using the potential (2.3) and the potential (2.3) plus the contribution of the 16 next neighboring strings, respectively, are presented. We see no changes in the wave function.

The scheme of the transverse motion energy levels for the channeling electrons is presented in figure 2 (a). The electromagnetic transitions from upper to lower energy levels produce the channeling radiation (CR). We calculate CR spectrum using dipole approximation formulae [12]. The contribution of the given transition $|i\rangle \to |f\rangle$ to the radiation spectrum is taken into account if the dipole moment of the transition exceeds some threshold, namely

$$\left|\boldsymbol{\rho}_{fi}\right| = \left| \int \psi_{\perp}^{(f)}(x,y)^{*}\, \boldsymbol{\rho}\, \psi_{\perp}^{(i)}(x,y)\, dxdy \right| \geq 10^{-2}\ \text{Å} \tag{3.3}$$

(where $\boldsymbol{\rho} = x\mathbf{e}_x + y\mathbf{e}_y$ is the radius vector in the (x, y) plane); remember that the elementary cell size over which the integration is performed in (3.3) amounts $a \approx 1.92$ Å. The introduction of the threshold permits to exclude from the consideration the artifacts connected to numerical errors.

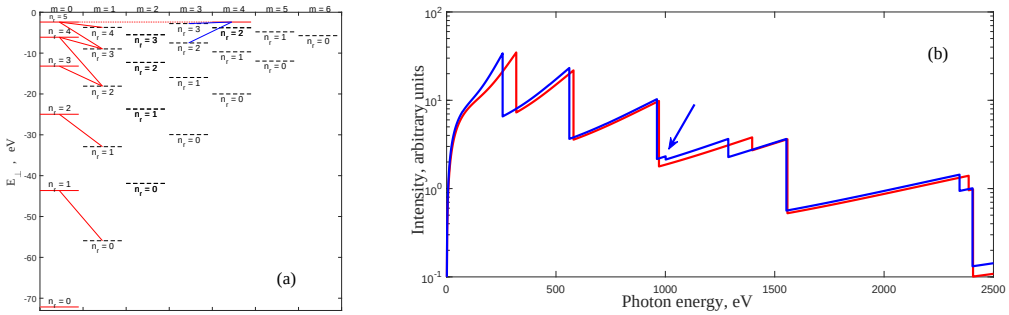

Figure 2. (a) Levels of transverse motion energy of $E_{\|} = 50$ MeV electrons channeling in (2.3) potential. Red bars mark the levels populated in the case of zero incidence angle of the beam to [100] axis. The transitions from them that meet the (3.3) criterion are shown by red and blue lines, the last ones are the additional transitions possible due to violation of axial symmetry in the potential (2.3). (b) Corresponding CR spectra of electrons in the potentials (2.2) (red line) and (2.3) (blue line).

The CR spectra in figure 2 (b) are computed for the simplest case of thin crystal (allowing to neglect the kinetics of the levels population during the beam travel through the crystal [12]) and zero angle of the beam incidence to [100] axis (hence only the states with $m = 0$ are initially populated with electrons). CR spectrum is determined by the orbital momentum selection rule: in dipole approximation only the transitions with $\Delta m = \pm 1$ are permitted. The difference between CR spectra in the potentials (2.2) and (2.3) is due to the fact outlined above: the highest initially populated level in the potential of the single string (2.2) is the pure state $|n_r = 5, m = 0\rangle$, so the transitions only to the states with $m = 1$ are permitted. In contrary, the analogous state in the potential (2.3) is the superposition of $m = 0$ and $m = 4$ states (see figure 1 (b)), so the additional transitions from the upper state to the states with $m = 3$ and $m = 5$ become possible. These additional transitions are marked in figure 2 (a) by blue lines; the probability of one among them, to the state $|n_r = 2, m = 3\rangle$, is enough to manifest itself in CR spectrum (the additional peak due to this transition is pointed in figure 2 (b) by the arrow). So, violation of the axial symmetry of the potential that leads to chaotization of the motion can manifest itself in additional peaks in CR spectrum.

2018 JINST 13 C01017

The potential well for the channeling positrons (2.4) could not be considered as a slightly perturbed axially symmetric well. However, it also possesses the symmetry of the square, hence the stationary states of the channeling positrons also can be classified via irreducible representations of D_4 group. The computed eigenfunctions of the channeling positron of the energy $E_{\parallel} = 1$ GeV are presented in figure 3 (for the twice degenerated states only one of the eigenfunctions is pictured; the second one can get by rotation on 90 degrees). Remember the qualitative distinctions between the wave functions in the regular and chaotic cases studied by various authors (see, e.g., [3–5, 7]):

(i) the nodal lines of the regular wave function exhibit crossings (in separable case) or tiny quasi-crossings (in non-separable, but still regular case) forming checkerboard-like pattern; those of the chaotic wave function form a sophisticated pattern of black and white "islands", the nodal lines quasi-crossings have significantly larger avoidance ranges;

(ii) near the classical turning line the nodal structure of the regular wave function immediately switches to the straight nodal lines, in the outer domain going to infinity; for the chaotic wave function an intermediate region exists outside the turning line, where some of the nodal lines pinch-off, making transition to the classically forbidden region more graduate and not so manifesting in the nodal structure. We see both of these features in the wave functions in figure 3.

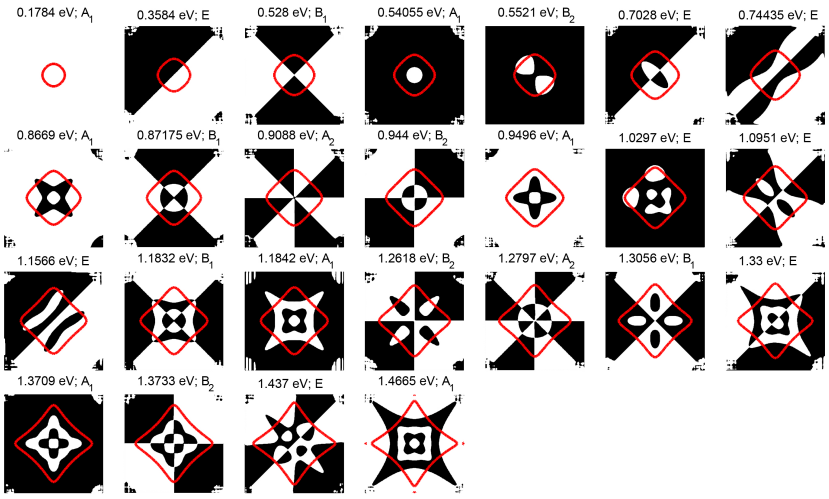

Figure 3. The transverse motion eigenfunctions of $E_{\parallel} = 1$ GeV positron channeling along [100] direction of Si crystal. Red lines are the classical turning lines $U^{(+)}(x, y) = E_{\perp}$.

The manifestations of chaos in quantum systems are found also in the statistical properties of their energy spectra. Consider the distances s between consequent levels in the spectrum of $E_{\perp}$ eigenvalues. The unfolding procedure [6] leads to dimensionless values of s with the average inter-level spacing $D = 1$ for the $E_{\perp}$ range under consideration. The quantum chaos theory predicts (see, e.g., [3–6]) that the energy levels nearest-neighbor distribution of the chaotic system obeys Wigner function

$$p_W(s) = (\pi s/2)\exp(-\pi s^2/4) \tag{3.4}$$

while the regular system — the exponential one (frequently referred as Poisson distribution)

$$p_P(s) = \exp(-s)\,. \tag{3.5}$$

2018 JINST 13 C01017

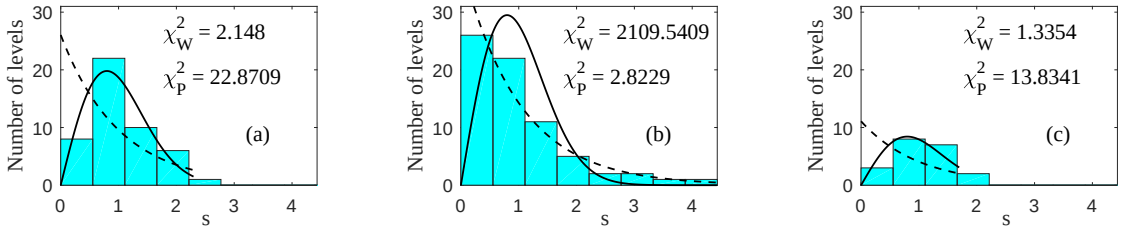

Figure 4. Nearest-neighbor spacing distribution for the $E_{\|} = 5\,\text{GeV}$ channeling electrons in the interval $-3 \le E_{\perp} \le -2\,\text{eV}$ (a) and $-5 \le E_{\perp} \le -3\,\text{eV}$ (b) in comparison with Wigner (3.4) and Poisson (3.5) distributions (solid and dashed lines, respectively), and for the channeling $E_{\|} = 4\,\text{GeV}$ positrons (c).

The histograms for the type A_1 level spacing of $E_{\|} = 5\,\text{GeV}$ channeling electron are presented in figure 4 for the intervals $-3 \le E_{\perp} \le -2\,\text{eV}$ (a) and $-5 \le E_{\perp} \le -3\,\text{eV}$ (b). We see that in the first case the distribution is close to Wigner one (that is confirmed by the χ^2 values calculated for both hypotheses, Wigner and Poisson). This result is in agreement with the fact that the domain of chaotic dynamics of the system occupies substantial part of the phase space, $\sim 40\%$ (estimated using Poincaré sections). The level spacing distribution in the second case is closer to (3.5) rather than to (3.4) that is due to mainly regular dynamics of the channeling electron in this $E_{\perp}$ range (regular trajectories occupy $\sim 90\%$ of the phase space). The A_1 level spacing of $E_{\|} = 4\,\text{GeV}$ positrons (which motion is mostly chaotic) is also obeys Wigner distribution (figure 4 (c)).

4 Conclusion

The channeling of electrons and positrons near [100] direction in Si crystal is considered from the quantum-mechanical viewpoint. The energy levels and wave functions of the particle's transverse motion in (100) plane as well as radiation transitions have been computed numerically. We see differences between motion and radiation characteristics in regular and chaotic cases. So, quantum chaos can manifest itself not only in semiclassical case (where the density of energy levels is high), but also in the case of small total number of energy levels.

Acknowledgments

This research is supported by the grant of Russian Science Foundation (project 15-12-10019).

References

[1] A.I. Akhiezer and N.F. Shul'ga, *High-energy electrodynamics in matter*, Gordon and Breach, (1996).

[2] U.I. Uggerhøj, *The interaction of relativistic particles with strong crystalline fields*, *Rev. Mod. Phys.* **77** (2005) 1131.

[3] R.M. Stratt, N.C. Handy and W.H. Miller, *On the quantum mechanical implications of classical ergodicity*, *J. Chem. Phys.* **71** (1979) 3311.

[4] M.C. Gutzwiller, *Chaos in classical and quantum mechanics*, Springer-Verlag, New York U.S.A., (1990).

2018 JINST 13 C01017

[5] V.P. Berezovoj, Yu.L. Bolotin and V.A. Cherkaskiy, *Signatures of quantum chaos in wave functions structure for multi-well 2D potentials*, *Phys. Lett.* **A 323** (2004) 218.

[6] L.E. Reichl, *The transition to chaos*, Springer, New York U.S.A., (2004).

[7] N.F. Shul'ga, V.V. Syshchenko, A.I. Tarnovsky and A. Yu. Isupov, *Structure of the channeling electrons wave functions under dynamical chaos conditions*, *Nucl. Instrum. Meth.* **B 370** (2016) 1 [arXiv:1512.07395].

[8] M.D. Feit, J.A. Fleck Jr. and F. Steiger, *Solution of the Schrödinger equation by a spectral method*, *J. Comput. Phys.* **47** (1982) 412.

[9] S. Dabagov and L.I. Ognev, *Passage of MeV-energy electrons through monocrystals*, *Nucl. Instrum. Meth.* **B 30** (1988) 185.

[10] L.D. Landau and E.M. Lifshitz, *Quantum mechanics. Non-relativistic theory*, Pergamon Press, Oxford U.K., (1977).

[11] J. Mathews and R.L. Walker, *Mathematical methods of physics*, W.A. Benjamin, (1971).

[12] V.A. Bazylev and N.K. Zhevago, *Radiation from fast particles in substance and in external fields* (in Russian), Nauka, Moscow Russia, (1987).

2018 JINST 13 C01017